Jordan Journal of Civil Engineering, Volume **2**, No. **4**, **2008**

Numerical and Experimental Investigation of a Reference Aluminium Bolted Joint

Evangelos Efthymiou [1)]

[1)] Institute of Metal Structures, Department of Civil Engineering, Aristotle University of Thessaloniki, GR-54124 Thessaloniki, Greece

ABSTRACT

In the herein presented paper the structural response of aluminium alloy bolted joints under tension is numerically and experimentally investigated. For the purpose of this research activity, the equivalent T-stub reference joint has been used and all special features of the employed structural aluminium have been incorporated into the mechanical model of the component. The proposed finite element model has been next calibrated with regard to test results obtained by an extensive laboratory programme. The aim of the aforementioned research effort was to contribute to the broadening of the knowledge on the behaviour of the aluminium bolted joints under tension by validating and calibrating the proposed numerical model comparing it with the results of a sequence of experimental tests.

Certain important aspects of the numerical treatment of the problem, namely, strain-hardening and contact phenomena, along with comparisons to relevant experimental results, are included in the paper. In addition, both the codified failure mechanisms described in Eurocode 9 and the possible theoretical yield patterns have been verified, whereas in the meantime useful conclusions concerning the development of post-elastic failure zones on aluminium flanges of the T-stub have been reached.

KEYWORDS: Aluminium alloy bolted joints, Equivalent T-stub component, Numerical analysis, Yield patterns, Experimental tests.

INTRODUCTION

In the latest years, the option of the use of structural aluminium in civil engineering applications is becoming a very attractive possibility, since its physical properties such as lightness and corrosion resistance, along with the extrudability of the material, which provides a wide range of structural typologies, make aluminium a very attractive structural material. Aluminium is, however, a relatively new material in the building and construction market and so many factors concerning its structural performance are not clear yet, and in many cases they are even unknown. This lack of knowledge on its structural performance is being mostly covered by Eurocode 9 (EN 1999-1-1), providing all specification and codified procedures and rules for the design of structural aluminium members. Eurocode 9 is the latest addition to the already existing Eurocode series and images a relatively short history of aluminium as a constructional material, comparable to steel. Despite a phenomenal resemblance of these two metals, the analysis tools and design methods could not be directly implemented in the case of structural calculations of aluminium members. The great variety of aluminium alloys, which affects mechanical properties of each alloy, along with issues regarding postelastic

Accepted for Publication on 1/10/2008.

behaviour of aluminium especially at the ultimate state, are parameters that prevent engineers from implementing standard and general application rules, and on the contrary require a specialised study as to every individual case. In addition, the constitutive law of alloyed aluminium differs a lot from the correspondent stress-strain curve $\sigma - \varepsilon$ in the case of steel, since there is no horizontal yield plateau and the behaviour is characterized by strain hardening and limited ductility. These issues along with some other critical ones, such as the buckling of slender aluminium elements and the reduction of strength, due to welding, have been investigated by many researchers in the past years towards the directions of understanding the structural performance of structural aluminium and its alloys. In addition, the subject of aluminium joint behaviour is one of the most important topics in structural analysis of metal structures along with stability and fatigue. However, the knowledge status research level regarding structural aluminium connections is far from the respective level regarding steel connections and the need for further research investigation is deeply felt.

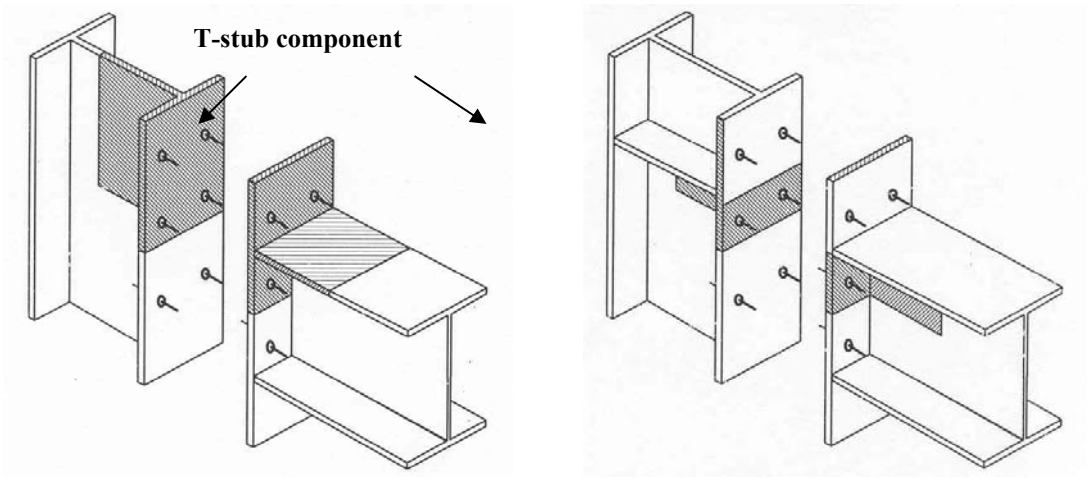

Figure (1): Equivalent T-stub component.

Structural Aluminium Connections-Framing of the Research Activity

Regarding structural aluminium connections, riveted and welded connections were the first to be investigated (Zygomalas et al., 2001), while aluminium bolted joints have just recently become a research subject, in contrast to bolted steel connections, which have been thoroughly analysed and investigated in the past decades by means of the T-stub idealization. The T-stub configuration represents the most efficient modelling tool for the resistance of components of bolted joints by simulating the strength of the basic parts of structural joints, following the requirements of Eurocodes 3 and 9 (prEN 1999-1-1, 2004; prEN 1993-1-8, 2002). Within this framework, the T-stub approach is the simplest way of evaluating the basic components of joint response in terms of strength, stiffness and ductility. It consists of two T-section components, whose flanges are connected to each other by means of one or more series of bolt rows and its static behaviour is determined by both tensile strength of the bolts and flexural resistance of the flange (Fig.1). In comparison to other types of connections, the T-stub is very efficient regarding ductility due to the yielding of the flanges in bending even in the case of members with low stiffness. Due to its great importance for the analysis of bolted metal connections, steel mechanical behaviour was examined in detail both numerically and experimentally (Stavroulakis et al.,

1995; Faella et al., 1998; Bursi and Jaspart, 1997; Agreskov, 1976), where the structural response of steel bolted joints both in elastic and plastic range has been clarified and many calculation methods and design rules up to failure have been established.

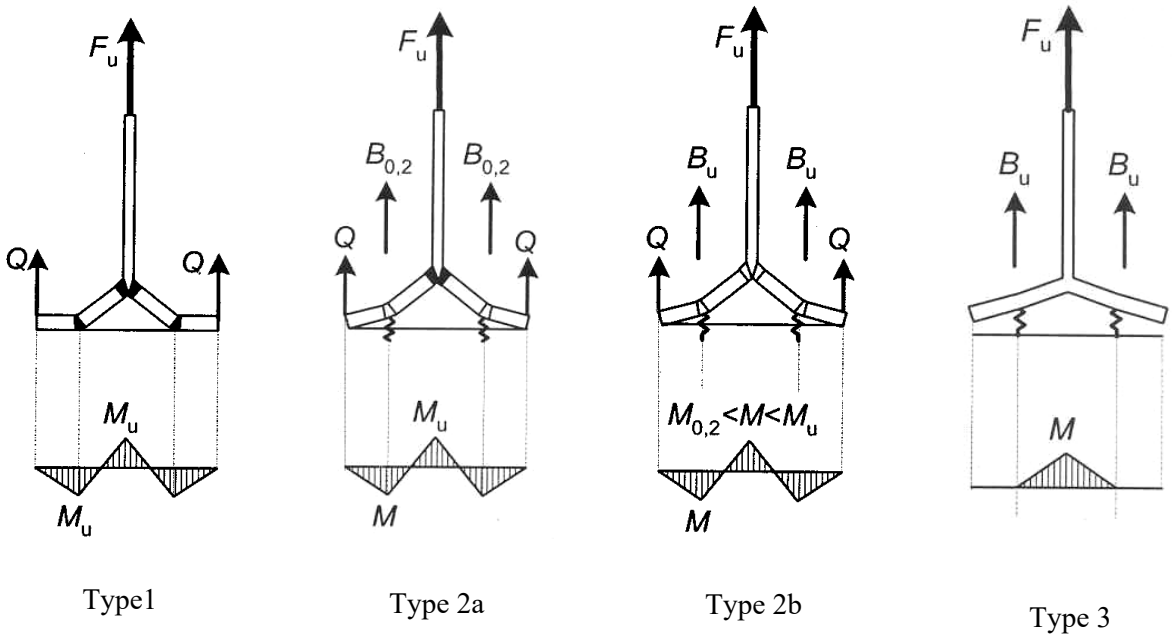

Figure (2): Failure modes of the aluminium T-stub.

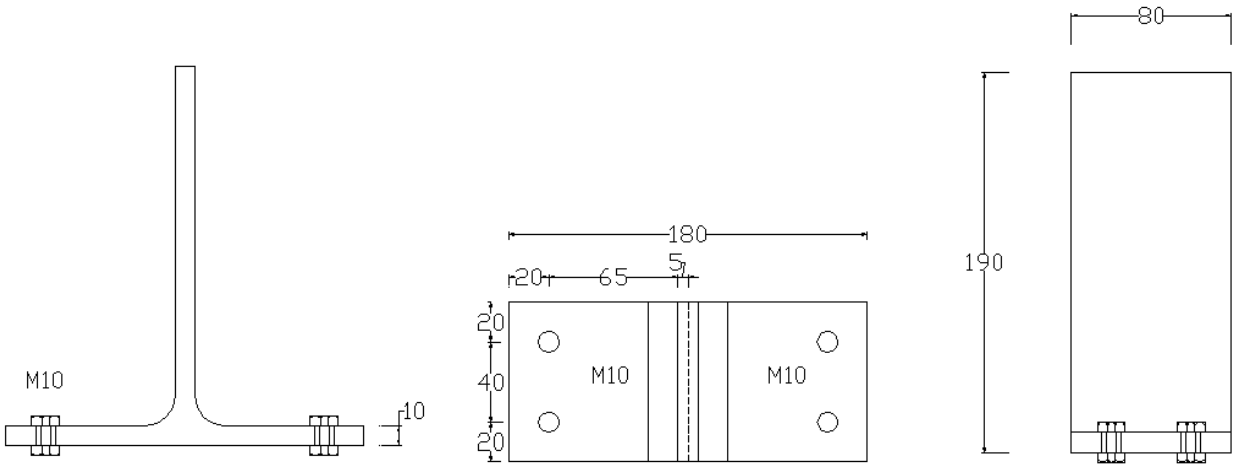

Figure (3): Geometrical Parameters of the Model.

In recent years, the possibility of applying the already existing rules and using calculation methods in the case of aluminium bolted aluminium joints was examined (De Matteis et al., 2001). Furthermore, researchers focused on the numerical investigation of their mechanical response (De Matteis et al., 1999; De Matteis et al., 1998; De

Matteis et al., 2000), supported by laboratory tests. The basic objectives were a parametrical analysis of aluminium connections and a correspondent experimental validation. In order to clarify all these issues regarding the structural performance of aluminium connections and to exploit all the advantages of aluminium in civil engineering projects, further research must be carried out.

This paper aims at examining numerically the bolted aluminium alloy T-stub joint under tension by applying the finite element analysis and calibrating the proposed model by the results from a series of laboratory tests that were carried out at the Laboratory of Steel Structures, Aristotle University of Thessaloniki. The configuration of the specimens was based on the requirements of Eurocode 9, while the experimental results can be obviously used as a basis for further investigation.

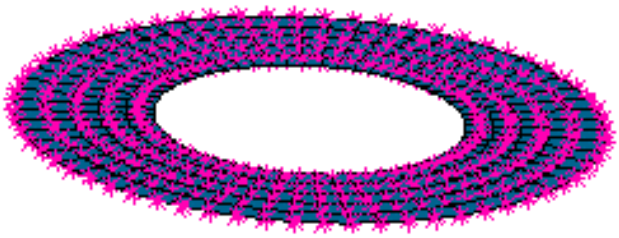

Figure (4): Contact elements.

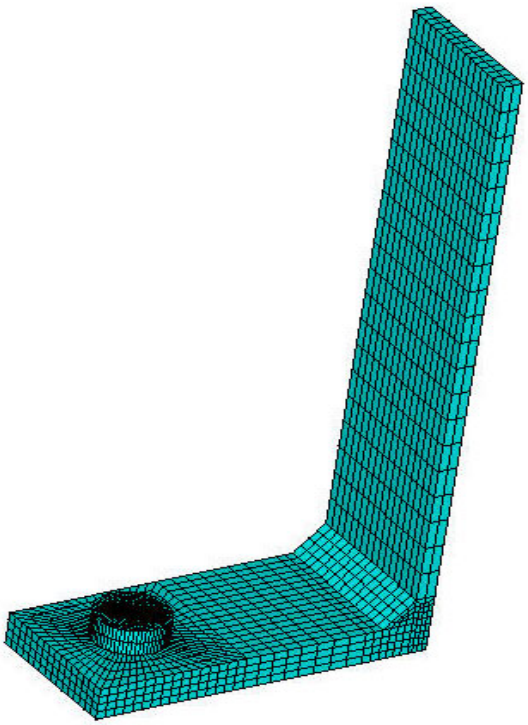

Figure (5): T-stub finite element model.

In addition, an investigation into the development of "yield-like" lines on aluminium flanges taking into account theoretical provisions and the calibration of the numerical model by means of the experimental results are

objectives of this research and all phenomena developed in the elastic and the post-elastic range have also been analyzed. Special features of structural aluminium have been incorporated in the numerical model, namely, strain hardening and relatively low ductility, and great emphasis has been given on the contact conditions between bolts and aluminium flanges.

Numerical Study of the Aluminium T-stub Joint Structural Response

On the Failure Mechanisms

As mentioned previously, in case of the calculation of bolted connections, the T-stub approach is adopted, where the ultimate resistance of components through collapse mechanisms (failure mechanisms) and the developing yield lines are evaluated. According to this approach, the flange of a column is replaced by a T-stub flange having a specific length, the effective length, and design equations based on the yield line analysis are provided (Baniotopoulos, 2003). The basic concept of the non-linear approach of the yield line analysis, which was originally introduced for concrete slabs and later extended to steel plates, was the observation of behavioural aspects of the structure gradually up to a collapse. Generally, tension is rising during the loading phase and a discrete point on the plate is recognized, where further increase in bending moments beyond maximum will cause a dispersion of yielding in the adjacent points, whereas yield zones, which can be idealized as yield lines, are developed. The analysis of the structure by means of yield lines includes firstly the assumption of yield line patterns and the evaluation of all possible collapse mechanisms, which are based upon boundary conditions and loading cases. Then, the ultimate load of the system is determined as the lowest value of all possible yield patterns.

In case of aluminium bolted connections and in Eurocode 9-Annex B paricularly, the characteristics of an equivalent aluminium T-stub joint are presented as well as the expressions of effective length determination. The mechanical behaviour of an equivalent aluminium T-stub is determined by the flexural resistance of flanges and the tensile strength of bolts. According to Eurocode 9 - Annex B there are three basic failure mechanisms regarding the case of aluminium T-stubs (Fig. 2). Type-1 mechanism is characterized by a complete yielding of the flange and the development of four hardening plastic hinges, two of which are located at bolt axes and the other two are formulated along the strip in the flange-to-web connection. In comparison to the steel T-stub, the difference is that the second failure mode is subdivided into categories dependent on the aluminium alloy properties and the developing prying forces. The collapse may be attained in either the bolt or the flange depending on the ultimate deformation capacity or the deformation gradient of the members. Type-2a mechanism occurs when there is a flange failure and a simultaneous development of two hardening plastic hinges with bolt forces at the elastic limit, while type-2b mechanism is determined by a bolt failure with yielding of the flange at the elastic limit. The ideal situation, with both entities, i.e. steel bolt and aluminium flange yield at the same time is not further taken into account because it never occurs in practical applications. Finally, in the case of failure mode 3, a bolt failure is recognized without flange yielding occurring.

The governing parameters of this failure mechanism concept are geometrical configuration, the tension resistance of the bolt-assembly B_u and the bending plastic resistance of the flange section M_u being calculated with respect to effective length (Johannsen, 1962). It is noteworthy that in the case of the aluminium T-stub flange, low material ductility can limit plastic deformation and, therefore, can influence the equilibrium condition at failure. In addition, the strain hardening characteristic of the alloy can lead to a different distribution of bending moment along the T-stub flange, due to the increase in moment at plastic hinge locations after first yielding.

Numerical Analysis

The numerical analysis presented in this paper was concerned with the study of the behaviour of the aluminium T-stub subjected to tensile force and carried

out by means of a general non-linear finite element code. The proposed three-dimensional model included special features of structural aluminium and emphasis has been given on the non-linear parameters of the problem. The geometrical model presented in Fig. 3 is a typical T-stub joint connected to a rigid steel base by a group of four M10 with the grade of 8.8 bolts. This configuration simulates the connection between members having different stiffness at beam-to-column joints. The T-stub components are plate elements with a throat of thickness $a = 8mm$; both the flanges and the web have a common thickness of $t = 10\ mm$. In particular, the geometrical parameters are as follows:

- Length $l = 180\ mm$.
- Width $b = 80\ mm$.
- Height $h = 190\ mm$.
- Height of the nut, m=8mm.

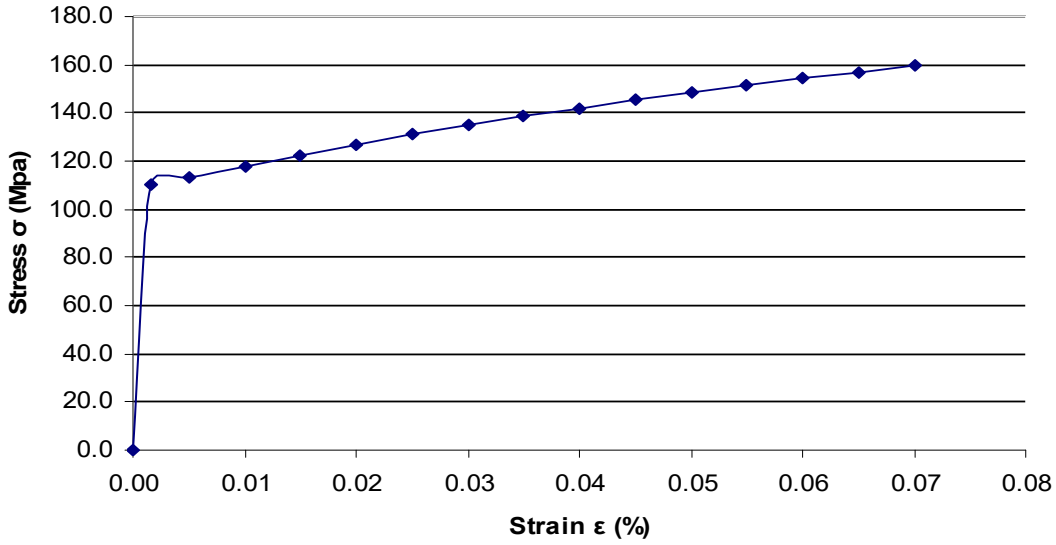

(a)

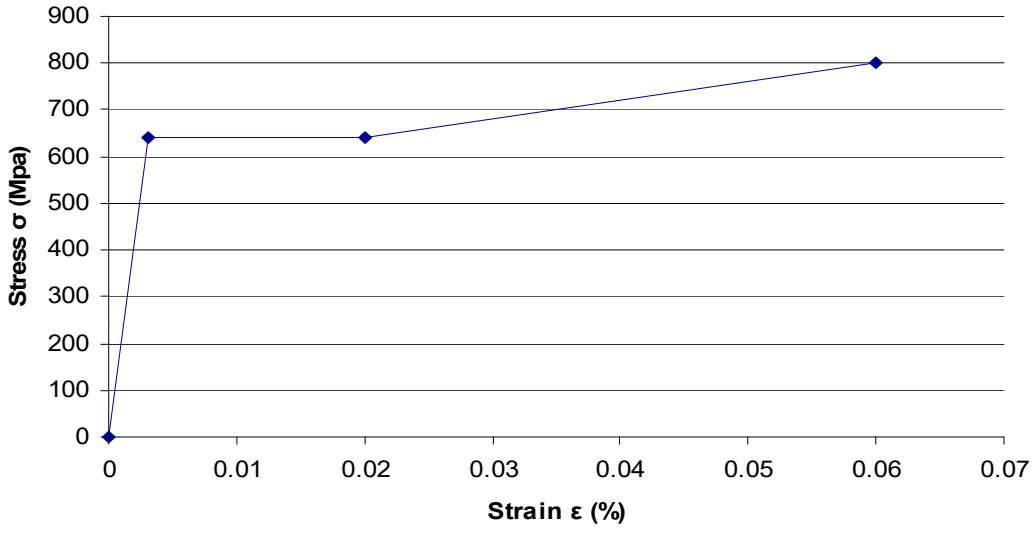

(b)

Figure (6): Stress-strain diagrams of aluminium and steel members.

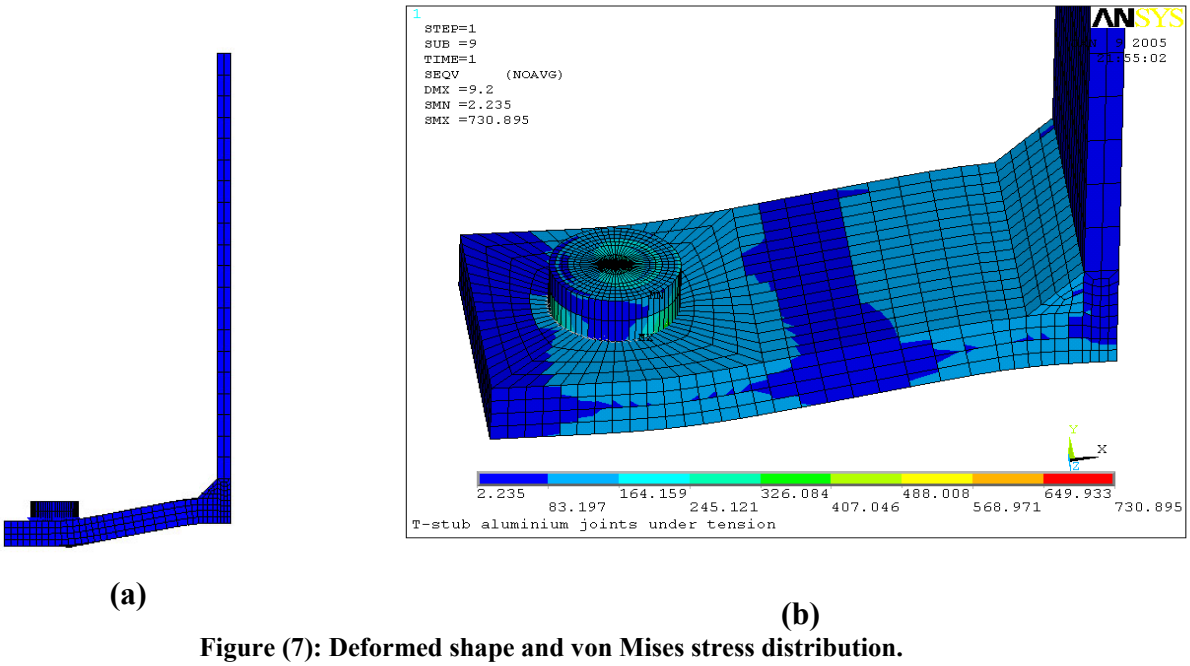

(a) **(b)**

Figure (7): Deformed shape and von Mises stress distribution.

Due to the symmetry of the T-stub structure, only a quarter of the model was considered by applying the appropriate boundary conditions. For simplification purposes in the analysis and economy in the cpu time, both the threaded part of the bolt shank and the washer were neglected.

The element used for the simulation of both aluminium components, namely, the flanges and the web, as well as for the steel bolts was the solid eight-node element SOLID45. This element has 3 degrees of freedom, namely u_x, u_y and u_z in each node, while it supports both plasticity and large strain. Special contact elements have been used in order to simulate the non-linear interaction between the two different bodies, namely the aluminium flange and the steel bolts (Fig.4). The coefficient of friction in this region between bolt head and upper flange surface was $\mu=0.1$, while zero friction was considered between the aluminium flange and the rigid surface in order to simulate symmetrical behaviour. In its final form, the three-dimensional finite element model consisted of 6172 elements and 7499 nodes (Fig. 5).

Due to the fact that the problem is characterised by a large deformation, true stress and true strain have been used according to the material data provided by the finite element software. The relevant mathematical expressions were as follows:

$$\varepsilon_{true} = ln(1+\varepsilon_{eng}) \quad (1)$$

$$\sigma_{true} = \sigma_{nom}(1+\varepsilon_{eng}) \quad (2)$$

As a matter of fact, in large strain solutions all stress-strain input will be in terms of true stress and true (or logarithmic) strain. In order to convert strain from small (engineering) strain to logarithmic one, the formula $\varepsilon = ln(1+\varepsilon_{eng})$ is used, whereas to convert from engineering stress to true stress, the expression is $\sigma_{true} = \sigma_{eng}(1+\varepsilon_{eng})$ (Hinton, 1992). The solution was displacement-based, namely a displacement was applied on the top of the web and the method that was used for solving this non-linear problem numerically was the *Newton-Raphson* method.

The T-stub plate elements are made of AW 6063-T5, which is an aluminium heat treatable wrought alloy. The T5 condition (temper) refers to the procedure of the material being cooled from an elevated temperature shaping process and then artificially aged to the artificial aging that it is subjected to. It exhibits excellent

weldability and combines sufficient strength and good corrosion resistance. The minimum value of 0.2% proof stress (elastic limit) is $f_{0.2}$ =110 MPa, while its ultimate stress f_u is equal to 160 MPa and the elongation at rupture (ultimate elongation) is ε_t=7%. The modulus of elasticity of aluminium is $E = 70$ kN/mm^2 and its density is ρ=2700 kg/cm^3.

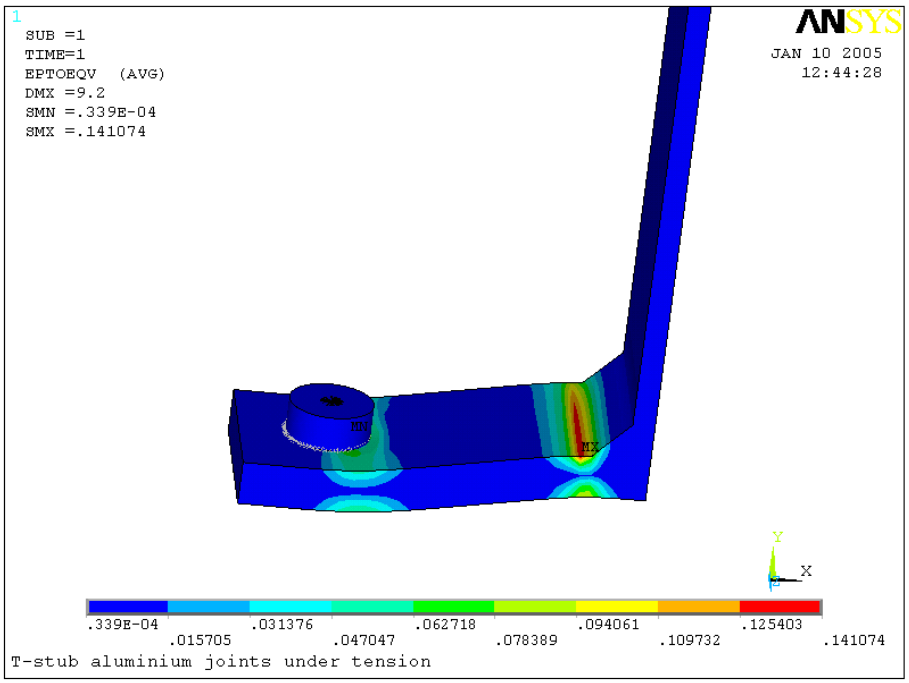

Figure (8): Inelastic strain zones.

In the case of aluminium, material behaviour can be described in a way, which differs from the elastic-perfectly plastic model that is used for steel. The constant strain hardening and a relatively low ductility of the alloy, which is dependent on the type of alloy, are the main factors that complicate the idealization of material properties (Efthymiou, 2005). In order to interpret the material mechanical behaviour, the exponential law of Hopperstad (Moen et al., 1994) was used for the description of the inelastic branch of the behaviour of aluminium T-stub members. This model defines that for stress values $\sigma \geq \sigma_o$ the following expression is valid:

$$\sigma = \sigma_0 + a\left[1 - exp\left(-\gamma\varepsilon_p\right)\right], \quad (3)$$

where ε_p is the plastic strain that corresponds to the stress value σ, σ_o is the characteristic value of the 0.2% proof strength and coincides with the elastic limit, whereas parameters a and γ determine the size of strain hardening and the shape of the curve, respectively. In particular, in the case of the aluminium alloy AW 6063-T5 parameter a is equal to 100 N/mm^2, since it is characterized by medium-to-low strain hardening and the factor γ =10. In Table 1, all relevant values are depicted, whereas in Figure 6a the stress-strain curve of AW 6063-T5 is presented. Concerning steel bolt idealization, a typical three-linear hardening model was used (Fig. 6b).

According to Eurocode 9, since aluminium alloy is a weaker material than high strength steel bolts, a specific model should exhibit type 1 mechanism failure, where the flanges fully yield and four plastic hinges are being formulated at the sections corresponding to flange-to-web connection and along the bolt axis. The numerical analysis verified the codified informative material (cf. the deformed T-stub model presented in Fig. 7a).

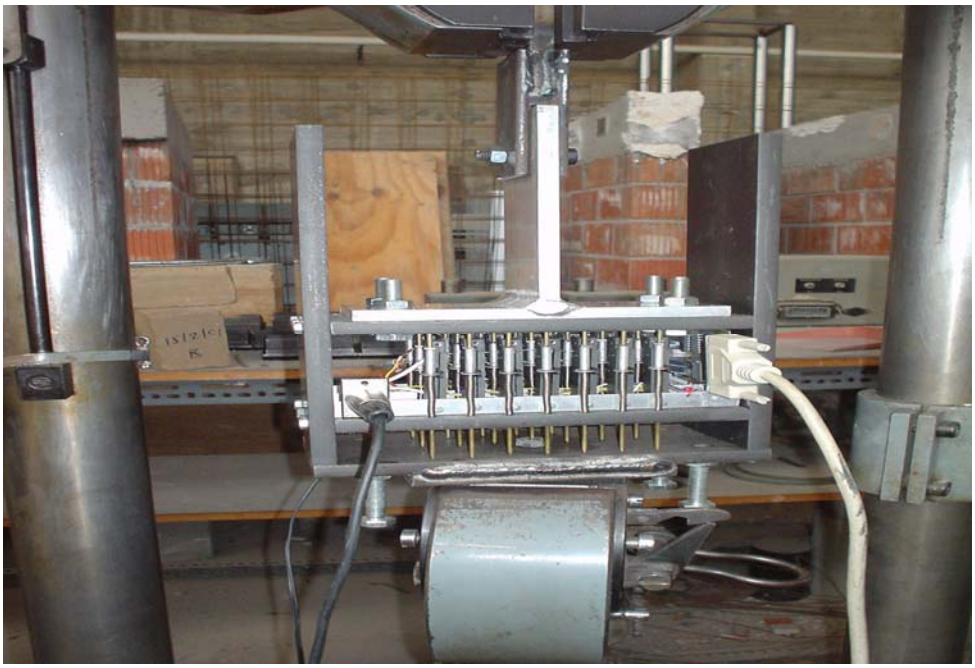

Figure (9): Experimental layout.

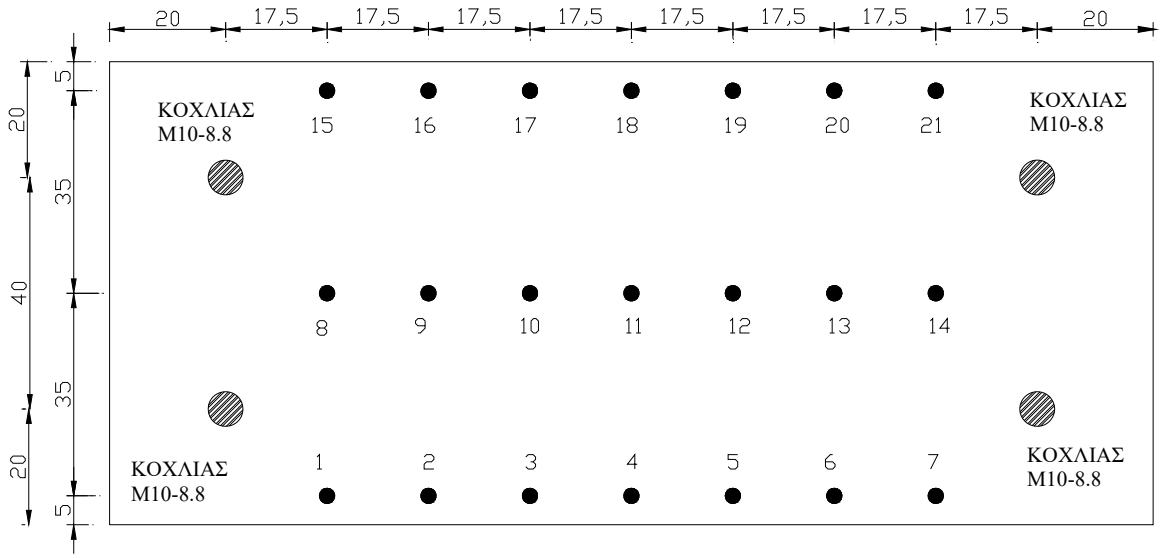

Figure 10: Measuring points.

The distribution of von Mises stresses on the T-stub is shown in Figure 7b, where along a large ratio of the flange area, the values of the developing stresses overcome the elastic limit of 110 MPa. The analysis provided total strains, both elastic and inelastic, that are coincident with the yield lines (and the location of plastic hinges), since they separate the flange from areas with elastic and inelastic behaviour. The lines which are extended to zones since the bolt material is particularly stiff comparable to aluminium flange material, have developed on the flange-

to-web connection and along the bolt axis (Fig. 8). The sum of elastic values of strain is negligible in comparison to the inelastic values. It is also noteworthy that along the yield lines the strain values beyond the ultimate strain values ε_{ult} can be observed, due to high strength bolts and strain-hardening effect that provided the possibility for the flange to deform beyond the ultimate strain. Also, the values of forces developing on the web were calculated and compared to the corresponding experimental results which are presented later.

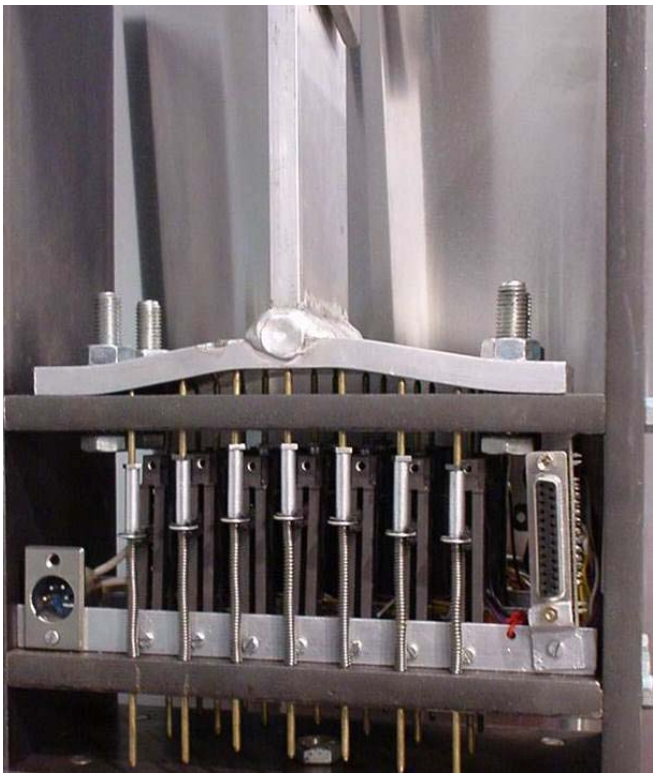

Figure (11): Deformed specimen.

It must be stressed that the term "plastic strains" is used conventionally in the previous paragraphs for the case of aluminium since aluminium is a hardening material without a stable yield plateau and clear observation of plastification behaviour, however, its stress-strain curve is characterized by a constant slope.

Experimental Tests

In order to validate the aforementioned numerical model and to create a calibration basis for further research on aluminium alloy T-stub joints, a series of laboratory tests was carried out at the Institute of Steel Structures at Aristotle University of Thessaloniki. This experimental study is the first conducted in Greece, aiming at supplementing the existing worldwide experimental results regarding the structural response of aluminium T-stub joints under tension.

The T-stub plate elements were made of AW 6063-T5. The choice of this alloy was based on its frequent use in Greek construction works for structural purposes and its availability in the aluminium industry market. It exhibits excellent weldability and combines sufficient strength and good corrosion resistance. The extruded plates were connected by means of the MIG fillet welding process with a throat of thickness of $a = 8mm$ and filler metal AW 5356. A total number of 15 T-stub specimens were manufactured having the same geometrical characteristics as the model described in the numerical procedure.

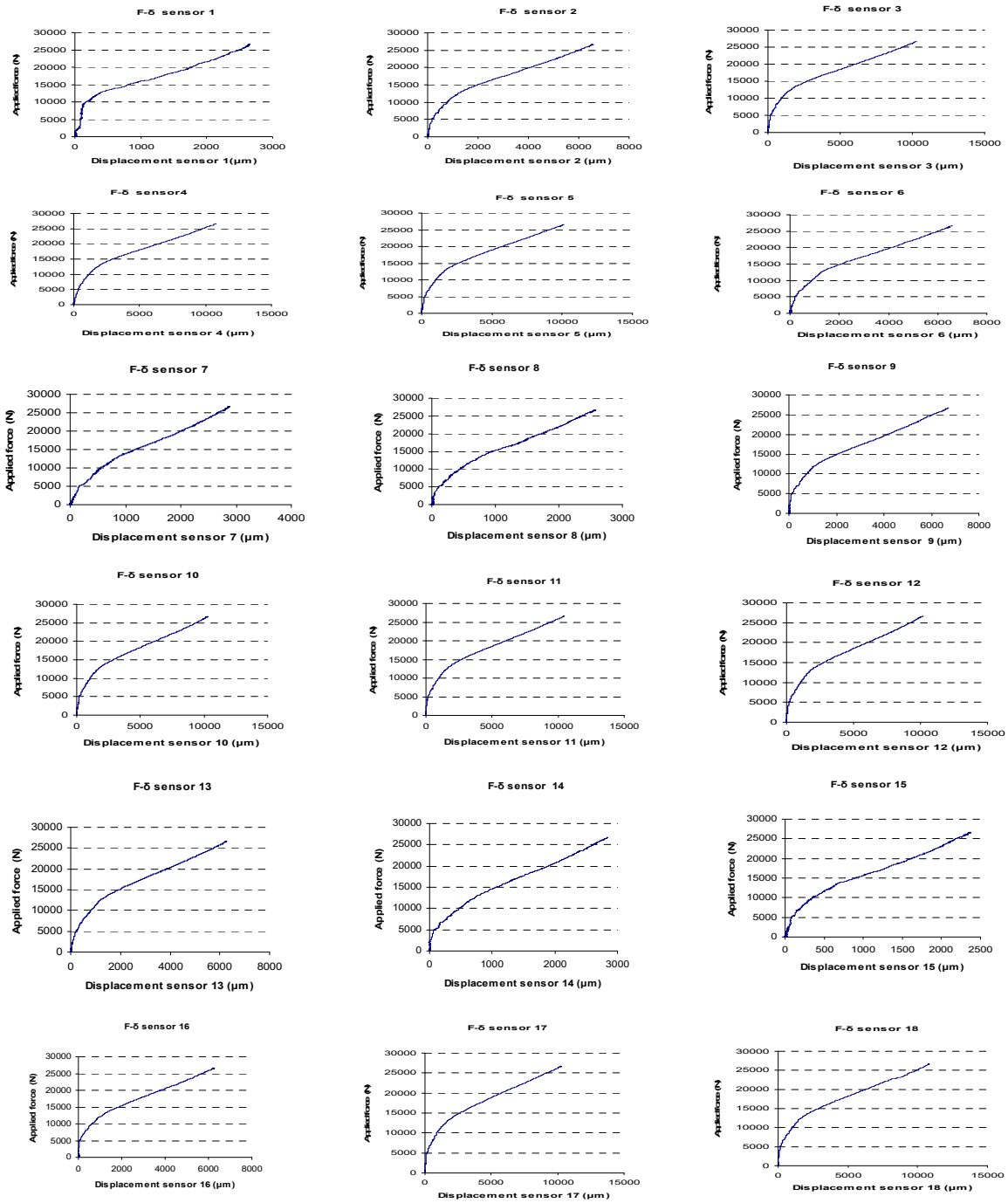

Fig. (12): to be continued

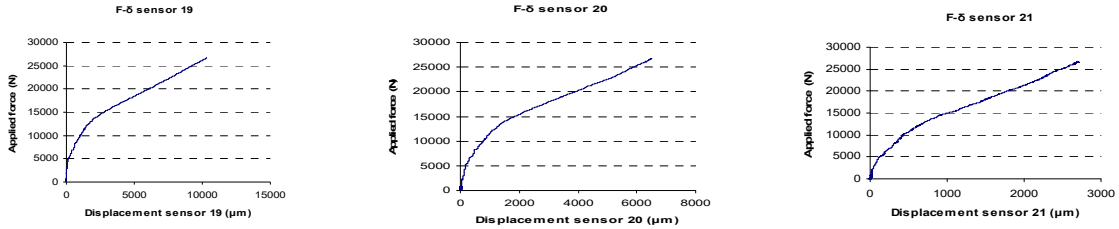

Figure (12): Force-displacement curves for experiment 5 (max. displacement).

Sensors	Numerical value (mm)	Experimental value (mm)	Difference
8	2.046	2.239	8.62%
9	5.29	5.838	9.39%
10	8.331	8.882	6.20%
11	9.108	9.063	-0.50%

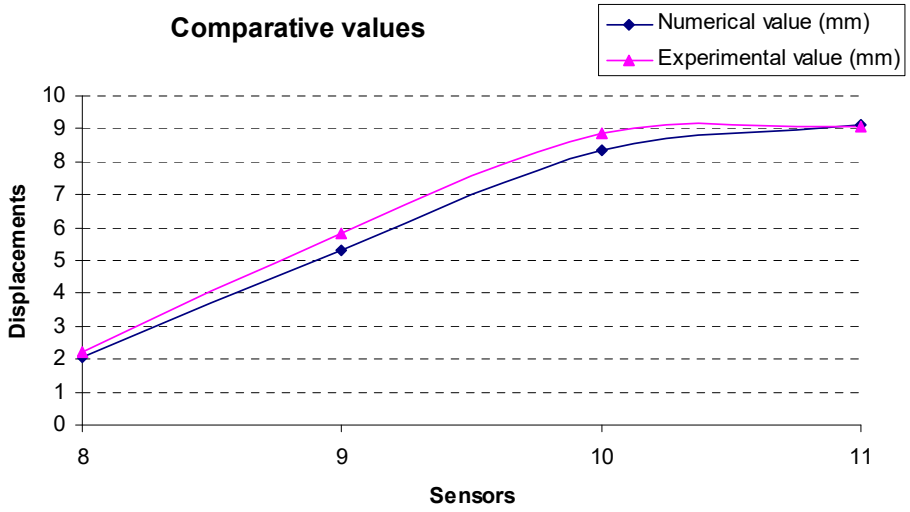

Figure (13): Comparison of the numerical results with respect to displacements (sensors 8-11).

The experimental layout consists of a test machine, T-stub specimens and a displacement measuring device, which was manufactured for recording displacements of the flanges (Fig. 9). This device is very sensitive and is able to measure displacements of the flanges by means of recording electricity through sensors being in contact with the flange on several points and, in particular, in 21 points distributed along the T-stub flanges (Fig. 10).

The aluminium T-stub component is joined to a steel plate, which is considered to be a rigid support due to its steel material features and its thickness. The assemblage was carried out by means of a two bolt row configuration through 4 high strength steel bolts M10 with a grade of 8.8, having yield strength f_{yb}=640 MPa and ultimate strength of f_u = 800 MPa. The bolt diameter is 10mm, while the hole diameter is 11mm. The displacement measuring device was connected to the undeformable metal plate so that the displacements in 21 points of the

flange by means of the respective sensors could be recorded. The experiments were force control conducted and the application of the tensile forces in the web of the T-stub was gradual and the range of maximum tensile values was between 21 and 27 kN, depending on the sensitivity specifications of the device and on the fact that a full response, both elastic and inelastic, should have been registered. The basic advantage was the possibility of a detailed description of the deformed situation of the aluminium T-stub joint by recording the displacements in 21 points for each test.

Sensors	Numerical value (mm)	Experimental value (mm)	Difference
15	2.028	2.162	6.20%
16	5.331	5.558	4.08%
17	8.487	8.743	2.93%
18	9.132	9.375	2.59%

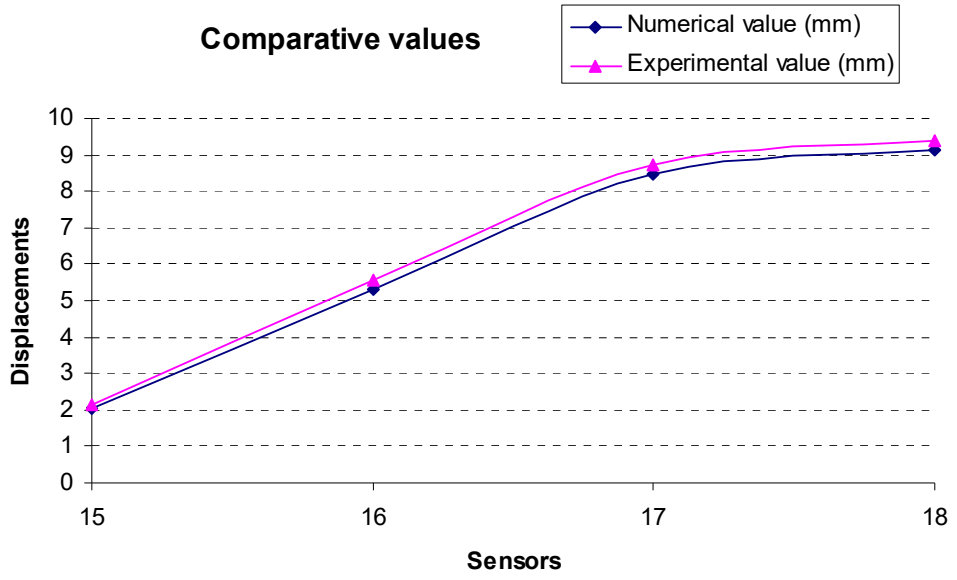

Figure (14): Comparison of the numerical results with respect to displacements (sensors 15-18).

The experimental programme was implemented in all 15 T-stub specimens, and for each test 1000 measurements per sensor were recorded, according to the specifications of the measuring device. The resultant displacement values and the corresponding forces were registered in Table 1 and in a form of force-displacement curves ($F-\delta$) and a detailed description of the deformed joint was then possible (Fig.11). The force-displacement curves that correspond to the maximum displacement of all tests which was equal to 10.6 mm are presented in Fig. 12, where the applied force was F=26.631 kN. The average of the applied forces was equal to 21.992 kN, while the average of maximum displacement was 9.3 mm. Complete information is given in Table 2. It is noteworthy that there is a slight difference between the displacement values in each experiment. This was due to the fact that the applied forces were not equal to each other and not constant because of the special sensitivities of the measuring device, while material and geometrical imperfections at the fabrication stage influenced the results. In addition, the different tightening grade of the flanges and the steel rigid base in each T-stub specimen slightly influenced the final results.

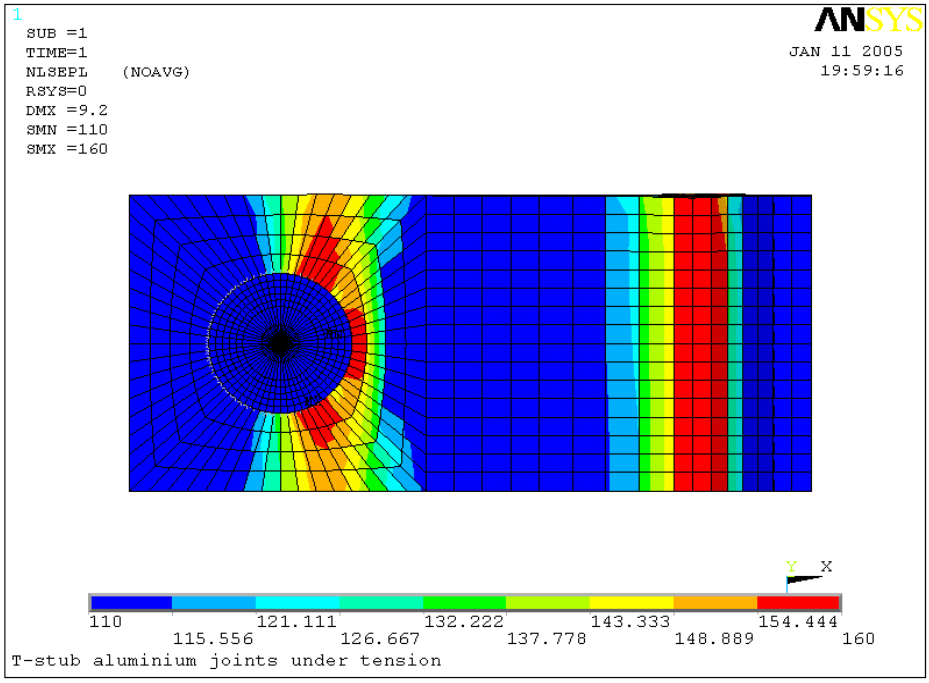

Figure (15): Yield zones on the T-stub.

Table (1): Stress-strain values of AW 6063-T5 alloy.

	σ_o (N/mm^2)	σ (N/mm^2)	ε	ε_p	σ/E
1	110.00000	0.00000	0.00000	0.00000	0.00000
2	110.00000	110.00000	0.00157	0.00000	0.00157
3	110.00000	113.37046	0.00500	0.00343	0.00162
4	110.00000	118.08314	0.01000	0.00843	0.00169
5	110.00000	122.56598	0.01500	0.01343	0.00175
6	110.00000	126.83019	0.02000	0.01843	0.00181
7	110.00000	130.88643	0.02500	0.02343	0.00187
8	110.00000	134.74484	0.03000	0.02843	0.00192
9	110.00000	138.41508	0.03500	0.03343	0.00198
10	110.00000	141.90632	0.04000	0.03843	0.00203
11	110.00000	145.22728	0.04500	0.04343	0.00207
12	110.00000	148.38629	0.05000	0.04843	0.00212
13	110.00000	151.39122	0.05500	0.05343	0.00216
14	110.00000	154.24961	0.06000	0.05843	0.00220
15	110.00000	156.96859	0.06500	0.06343	0.00224
16	110.00000	159.55496	0.07000	0.06843	0.00228

Table (2): Experimental results.

	Deflection of experiments 1-15 (μm)															
SENSORS	u_1	u_2	u_3	u_4	u_5	u_6	u_7	u_8	u_9	u_{10}	u_{11}	u_{12}	u_{13}	u_{14}	u_{15}	**Average (μm)**
1	2764.28	1789.633	3140.794	2800.025	2657.045	2237.637	2499.767	2116.104	2316.276	2442.575	2266.233	2387.766	1720.526	2845.302	1784.867	**2384.588667**
2	6231.52	3751.44	7386.88	6830.08	6574.88	5860.32	6052.88	5034.4	5820.88	5934.56	5489.12	5820.88	3802.48	7222.16	4343.04	**5743.701333**
3	9774.333	5666.28	12020.32	10566.79	10316.33	9330.885	9312.408	7717.227	9078.366	8985.981	8413.194	8979.822	5670.386	11285.34	6401.254	**8901.260533**
4	10156.62	6308.92	12430.36	11220.46	10806.26	9794.74	9701	8074.72	9489.54	9740.24	8896.58	9367.46	6117.08	11817.78	6786.34	**9380.54**
5	9867.312	5619.432	12040.39	11077.25	10131.58	9502.584	10.92	7132.944	8770.944	9480.744	8454.264	8884.512	5304.936	11590.49	6272.448	**8276.0496**
6	6637.522	4026.108	7763.721	7193.142	6573.412	6447.329	6310.561	4823.209	5898.12	6287.054	5983.6	6218.67	3857.285	7575.665	4425.727	**6001.408333**
7	2981.803	1963.346	3069.165	3170.321	2887.544	2715.119	2809.378	2209.339	2623.159	2788.687	2749.604	2774.893	1938.057	3473.789	1988.635	**2676.189267**
8	2646.728	1687.07	2797.907	2659.874	2580.998	2361.898	2285.213	2015.72	2274.258	2206.337	2074.877	2239.202	1562.183	2478.021	1724.317	**2239.6402**
9	6773.8	3933.6	7689.2	7059.8	6707.8	6292	6010.4	5137	5843.2	5737.6	5403.2	5849.8	3832.4	6974	4358.2	**5838.8**
10	9954.302	5723.034	11921.4	10501.78	10308.68	9657.222	9245.554	7830.18	9050.33	8793.568	8356.436	9113.99	5623.3	10648.2	6503.93	**8882.126133**
11	10144.664	5978.408	12295.54	10938.54	10474.92	9769.955	9333.853	7890.059	9145.44	9134.855	8442.596	9225.886	5658.741	11004.17	6507.658	**9063.018133**
12	9956.163	5890.14	12184.37	10748.36	10193.6	9789.504	9319.206	7533.9	8960.775	9289.527	8604.627	9237.018	5627.595	10942.42	6746.265	**9001.5646**
13	6269.97	3685.09	7656.48	6625.8	6276.105	6204.53	5836.43	4644.195	5564.445	5752.585	5490.825	5873.24	3562.39	6762.815	4292.455	**5633.157**
14	2974.33	1816.128	3096.246	2877.638	2839.802	2738.906	2623.296	2120.918	2505.584	2507.686	2413.096	2642.214	1723.64	2951.208	1994.798	**2521.699333**
15	2805.801	1601.827	2757.892	2680.821	2376.703	2528.762	2191.316	1989.265	2130.909	2020.51	1920.526	2166.32	1466.432	2178.818	1624.74	**2162.709467**
16	6744.726	3582.654	7502.214	6821.796	6297.72	6308.73	5740.614	4921.47	5533.626	5364.072	5135.064	5689.968	3413.1	6262.488	4053.882	**5558.1416**
17	10039.68	5367.04	12472.32	10572.8	10248	9813.44	9087.68	7602.56	8783.04	8301.44	8010.24	9103.36	5228.16	10312.96	6209.28	**8743.466667**
18	10665.984	6114.688	12767.04	11152.06	10846.53	10414.02	9648.192	8209.792	9586.688	9267.264	8745.472	9856.512	5700.032	10812.8	6844.8	**9375.458133**
19	9630.82	5778.935	12468.24	10709.53	10335.19	9839.03	8933.095	7415.82	8764.755	8800.195	8168.92	9092.575	5389.095	10270.96	6565.26	**8810.827**
20	6424.136	3573.28	8008.808	6505.7	6490.164	6441.614	5742.494	4816.16	5627.916	5596.844	5400.702	5919.216	3412.094	6410.542	4363.674	**5297.084**
21	2889.108	1674.468	3060.459	2624.49	2713.419	2765.475	2368.548	2095.254	2362.041	2225.394	2153.817	2496.519	1533.483	2427.111	1941.255	**2355.3894**
Fmax (N)	**21127.1**	**22246.84**	**24920.28**	**24208.5**	**26691**	**22845.75**	**22377.05**	**20745.2**	**20745.2**	**21266**	**22758.95**	**21552.45**	**20779.9**	**22116.65**	**21248.65**	

CONCLUSIONS

Regarding the calibration of the numerical results based on the experimental results, the comparative displacement values are presented in Figures 12-13. The difference between the results concerning the displacements is small enough and, therefore, the numerical model of the T-stub presented herein has been verified. By means of this comparison, a satisfactory coincidence has been observed, as the displacement values of the sensors and the correspondent nodes differ from each other about 8% justified due to the simplifications in the numerical analysis and the parameters of the experimental procedure.

According to the yield line theory and its implementation in metal plates' behaviour, inelastic deformations take place along the yield lines and the numerical analysis pointed out that the elastic values of deformations are negligible in comparison to the inelastic values. In the particular model at hand, type 1 mechanism required by Eurocode 9 in the case of aluminium has been verified. This model consists of a development of post elastic failure zones on the aluminium flange, which determine the yield lines. Two basic yield lines are developed (Fig. 15):

- The first one appears in the area of the flange-to-web connection
- The second one has been developed along the bolt axis.

The inelastic type 1 mechanism defined by Eurocode 9 for aluminium plates has been verified and is similar to the corresponding mechanism of Eurocode 3 for steel. It is noteworthy that in the case of aluminium and as the bolt is particularly stiff comparable to aluminium material AW 6063-T5, these zones extend beyond the bolt axis giving rise to the development of wider failure regions.

The applied and presented finite element model of the aluminium T-stub described the properties of the structure to a sufficient degree and led to reliable results. As the numerical simulation pointed out, by increasing the force during experimental testing, aluminium enters the post-elastic behaviour branch very fast and deformations develop rapidly and are much larger than the theoretical ultimate deformations due to strain hardening.

ACKNOWLEDGEMENTS

The support of Assoc. Prof. Dr. M. Zygomalas, who is responsible for the testing facilities of the Institute of Metal Structures, Aristotle University of Thessaloniki, to the present research activity is gratefully acknowledged.

REFERENCES

Agreskov, H. 1976. High Strength Bolted Connections Subject To Prying, *Journal of Structural Division*, ASCE, 102, ST1, 161-175.

Baniotopoulos, C. C. 2003. *Structural Metal Connections in the Framework of Eurocodes 3 and 9*, Ziti Publications, Thessaloniki.

Bursi, O.S. and Jaspart, J.P. 1997. Benchmarks for Finite Element Modelling of Bolted Steel Connections, *Journal of Constructional Steel Research*, 43 (1-3): 17-42.

Bursi, O.S. and Jaspart, J.P. 1997. Calibration of a Finite Element Model for Isolated Bolted and End Plate Connections, *Journal of Constructional Steel Research*, 44 (3): 25-62.

De Matteis, G., Mandara, A. and Mazzolani, F.M. 2001. Calculation Methods for Aluminium T-stubs: A Revision of EC3-Annex J., *Proc. of 8th Int. Conf. on Joints in Aluminium (INALCO 2001)*, Munich.

De Matteis, G., Mandara, A. and Mazzolani, F.M. 1999. Remarks on the Use of EC3-Annex J for the Prediction of Aluminium Joint Behaviour, *Proc. of 6th Int. Conf. on Stability and Ductility of Steel Structures (SDSS'99)*, Timisoara.

De Matteis, G., Mandara, A. and Mazzolani, F.M. 1998. Numerical Analysis for T-stub Aluminium Alloy Joints, *Proc. of 4th Int. Conf. on Computational Structures Technology*, Edinburgh.

De Matteis, G., Mandara, A. and Mazzolani, F.M. 2000. T-stub Aluminium Joints: Influence of Behavioural Parameters, *Computers and Structures*, 78(1-3): 311-327.

De Matteis, G., Landolfo, R. and Mazzolani, F.M. 2001. Experimental Analysis of Aluminium T-stubs: Framing of the Research Activity, *Proc. of 8th Int. Conf. on Joints in Aluminium (INALCO 200),* Munich.

Efthymiou, E. 2005. *Development of Yield Lines in Aluminium Bolted Joints under Tension. A Numerical and an Experimental Approach*, Dissertation, Aristotle University, Thessaloniki.

Faella, C., Piluso, V. and Rizzano, G. 1998. Experimental Analysis of Bolted Connections: Snug Versus Preloaded Bolts, *J. Structural Engineering, ASCE*, 124 (7): 765-774.

Hinton, E. 1992. *NAFEMS Introduction to Nonlinear Finite Element Analysis*, Bell and Bain Ltd., Glasgow.

Johannsen, K.W. 1962. *Yield Line Theory*, Cement and Concrete Association, London.

Moen, L., Hopperstad, O.S. and Langseth, M. 1994. Elasto-viscoplastic Constitutive Models in the Explicit Finite Element Code LS-DYNA 3D, *Proc. LS-DYNA 3D Conf. Livermore Software Corporation,* Livermore, CA.

prEN 1993-1-1. 2002. *Part 1.8: Design of Joints,* CEN, Brussels.

prEN 1999-1-1. 2004. *Part 1.1: Design of Aluminium Structures: General Structural Rules,* CEN, Brussels.

Stavroulakis, G.E., Abdalla, K.M. and Panagiotopoulos, P.D. 1995. A Back-propagation Based Neural Network Approach for Modelling Semi-rigid Steel Structures Connections, *Proc. of Eurosteel '95,* Balkema, Rotterdam.

Zygomalas, M., Kontoleon, M.J. and Baniotopoulos, C.C. 2001. A Hemivariational Inequality Approach to the Resistance of Aluminium Riveted Connections, *Proc. of the 6th Greek Conf. on Mechanics*, Aristotle University, Thessaloniki.